Microglial glutamate release evoked by α-synuclein aggregates is prevented by dopamine

Mauricio Dos-Santos-Pereira, Leonardo Acuña, Sabah Hamadat, Jeremy Rocca, Florencia N González-Lizárraga, Rosana Chehín, Julia Sepulveda-Diaz, Elaine N Del-Bel, Rita Raisman-Vozari, Patrick P. Michel

Microglial glutamate release evoked by α-synuclein aggregates is prevented by dopamine

Running title: α-synuclein and microglial glutamate release

Mauricio dos-Santos-Pereira[1,2], Leonardo Acuña[1,3], Sabah Hamadat[1], Jeremy Rocca[1], Florencia González[1,4], Rosana Chehín[4], Julia Sepulveda-Diaz[1], Elaine Del-Bel[2], Rita Raisman-Vozari[1] and Patrick P. Michel[1]

[1]Institut du Cerveau et de la Moelle épinière (ICM), Inserm U 1127, CNRS UMR 7225, Sorbonne Université, F-75013 Paris, France

[2]Faculdade de Medicina de Ribeirão Preto, Universidade de São Paulo, Brazil

[3]Instituto de Patología Experimental (CONICET-UNSa), Salta, Argentina.

[4]Instituto de Medicina Molecular y Celular Aplicada (IMMCA) CONICET/UNT and SIPROSA, Tucumán, Argentina.

Correspondence: Patrick Pierre Michel, Institut du Cerveau et de la Moelle Epinière (ICM), Hôpital de la Pitié-Salpêtrière - 47, boulevard de l'Hôpital - 75013 Paris. patrick-pierre.michel@upmc.fr

Funding information: Program Investissements d'Avenir [ANR-10-IAIHU-06] and Translational Research Infrastructure for Biotherapies in Neurosciences [ANR-11-INBS-0011-NeurATRIS].

Total word count: 10055

Word count: Title page: 155; Abstract: 238; Keywords: 9; Main points: 27; Text: 6181; References: 2404; Figure legends: 1041.

Abstract: When activated, microglial cells have the potential not only to secrete typical proinflammatory mediators but also to release the neurotransmitter glutamate in amounts that may promote excitotoxicity. Here, we wished to determine the potential of the Parkinson's disease (PD) protein α-Synuclein (αS) to stimulate glutamate release using cultures of purified microglial cells. We established that glutamate release was robustly increased when microglial cultures were treated with fibrillary aggregates of αS but not with the native monomeric protein. Promotion of microglial glutamate release by αS aggregates (αSa) required concomitant engagement of TLR2 and P2X7 receptors. Downstream to cell surface receptors, the release process was mediated by activation of a signaling cascade sequentially involving phosphoinositide 3-kinase (PI3K) and NADPH oxidase, a reactive oxygen species-producing enzyme. Inhibition of the Xc- antiporter, a plasma membrane exchange system that imports extracellular L-cystine and exports intracellular glutamate, prevented the release of glutamate induced by αSa, indicating that system Xc- was the final effector element in the release process downstream to NADPH oxidase activation. Of interest, the stimulation of glutamate release by αSa was abrogated by dopamine through an antioxidant effect requiring D_1 dopamine receptor activation and PI3K inhibition. Altogether, present data suggest that the activation of microglial cells by αSa may possibly result in a toxic build-up of extracellular glutamate contributing to excitotoxic stress in PD. The deficit in dopamine that characterizes this disorder may further aggravate this process in a vicious circle mechanism.

Keywords: α-Synuclein, Glutamate, Microglia, Neuroinflammation, Parkinson.

Main points:

- Amyloid fibrils of α-Synuclein potently stimulated microglial glutamate release through activation of the Xc- antiporter.
- This effect was prevented through an antioxidant effect of dopamine.

Introduction

Parkinson disease (PD) is a multifactorial neurodegenerative disorder primarily characterized by a loss of midbrain substantia nigra dopamine (DA) neurons and ensuing motor deficits (Mullin and Schapira, 2015; Michel et al, 2016). Neuronal cell loss is probably the result of intrinsic mechanisms that affect neuronal function and ultimately neuronal viability. It is believed, however, that neurodegeneration is exacerbated by sustained inflammatory processes that implicate microglial cells (Hirsch et al, 2003; McGeer and Mc Geer, 2008), the resident immune cells of the brain (Ginhoux et al, 2010; Bohlen et al, 2017). Microglial activation in PD may not simply occur as a consequence of neuronal damage as originally thought but also as an intrinsic component of the disease process (Mouton-Liger et al, 2018).

Microglial cell activation was demonstrated in post-mortem tissue (Hirsch et al, 2003; McGeer and Mc Geer, 2008) and in living patients diagnosed with PD, using positron emission tomography imaging techniques (Ouchi et al. 2009; Bartels et al. 2010). The contribution of inflammatory processes in PD progression is also indirectly supported by epidemiological studies showing that the PD risk is reduced in long-term users of some nonsteroidal anti-inflammatory medications (Gagne and Power, 2010; Rees et al, 2011).

A number of studies suggest that the aggregation process which affects the synaptic protein α-Synuclein (αS), could represent a potential trigger for microglial cell activation (Zhang et al, 2005; Couch et al, 2011; Lema Tomé et al, 2013). Microglial activation may result from the presence of pathological αS aggregates that diffuse and propagate in the brain parenchyma of PD patients (Emmanouilidou et al, 2011; Dijkstra et al, 2014; Bernis et al, 2015) to finally form cytoplasmic inclusions, termed Lewy bodies, and abnormal neuritic depositions, termed Lewy neurites (Braak and Tredici, 2017). Consistent with this hypothesis, the extent of microglial activation estimated by HLA-DR immunostaining was reported to be closely correlated with the amount of αS deposited in the brain of PD patients (Croisier et al, 2005).

Here, our specific aim was to evaluate the pro-inflammatory potential of amyloid fibrils of αS, using glutamate release as a marker of the activation state of these cells. Our interest in this marker lies in the fact that activated microglial cells can release glutamate in amounts that have the propensity to promote excitotoxic stress (Mesci et

al, 2015), a glutamate-receptor-mediated process thought to contribute to PD neurodegeneration (Wallace et al, 2007; Ambrosi et al, 2014).

So, we established a model system of pure microglial cells in culture and used these cultures to evaluate the impact of αS aggregates (αSa) on glutamate release. We found that αSa had a strong stimulatory effect on glutamate release through a sequence of signaling events that ultimately lead to activation of the cystine/glutamate antiporter system Xc^-. Most interestingly, the stimulatory effect of αSa on glutamate release was totally suppressed by the neurotransmitter DA which operated through activation of D_1 DA receptors.

Materials and methods

Pharmacological and cell culture reagents

Lipopolysaccharide (LPS; Escherichia coli strain O26:B6; #L8274), 4',6-Diamidino-2-PhenylIndole (DAPI), sulfasalazine (Sulfa; #S0883); benzoylbenzoyl-ATP (BzATP; #B6396), dopamine (DA) hydrochloride (#H8502), SKF-81,297 hydrobromide (SKF; #S179), 2-bromo-α-ergocryptine methane sulfonate salt (ERG; #B2134), forskolin (FK; #F6886), trolox (TROL; #238813) were all purchased from Sigma Aldrich (L'Isle d'Abeau Chesnes, France). JNJ-47965567 (JNJ; #5299), LY294002 hydrochloride (LY; #1130) and diphenyliodonium (DPI; #0504) were from Tocris Bioscience. Apocynin (APO; #4663) was purchased from R&D Systems Europe. The Novex TNF mouse ELISA kit was from Thermofischer Scientific (Illkirch, France). The synthetic triacylated lipoprotein Pam3CSK4 (#vac-pms) was from Invivogen (Toulouse, France). Dulbecco's modified Eagle's medium (DMEM), DMEM/F-12 nutrient mixture, EDTA (2 mM)-Trypsin (0.05%), the Amplex Red Glutamic Acid/Glutamate Oxidase Assay Kit (#A12221) and the CellROX Deep Red Reagent were all purchased from Invitrogen Life Technologies (Saint Aubin, France). N5 medium which is not commercially available was prepared using reagents from Sigma-Aldrich (Kaufman and Barrett, 1983). Fetal bovine serum (FCS) and horse serum were obtained from Biowest LLC (Eurobio, Les Ulis, France) and Sigma Aldrich, respectively. Radioactive [^{14}C]-L-Cystine was obtained from Perkin Elmer (Courtaboeuf, France).

Primary antibodies

The MAC-1/CD-11b (clone M1/70.15, Cat# MCA74GA, RRID: AB_324660) antibody was from Bio-Rad/AbD Serotec (Oxford, UK) and the rabbit anti-ionized calcium binding adaptor molecule-1 (Iba-1; Cat# 019-19741, RRID: AB_839504) antibody from Wako Chemicals (Neuss, Germany). The rabbit polyclonal p47-phox antibody (Cat# sc-14015, RRID: AB_2150289) was from Cliniscience (Nanterre, France). The rabbit monoclonal antibody against AKT phosphorylated at Ser473 (p-AKT; Cat #4060, RRID: AB_2315049) and the rabbit polyclonal antibody against total AKT (Cat #9272, RRID: AB_329827) were both purchased from Cell Signaling Technology (Leiden, Netherlands). The rabbit polyclonal antibody against human αS (Cat# BML-SA3400, RRID: AB_2192956) was from Enzo Life Sciences (Lyon, France) and the polyclonal rabbit GADPH antibody (Cat# G9545, RRID: AB_796208) from Sigma Aldrich. The mouse monoclonal anti-Toll-like receptor (TLR)2-IgG antibody (Cat# mabg-mtlr2, RRID:AB_11125339), an antagonistic antibody for TLR2 was from Invivogen.

Production of glial cell cultures

Animal care and handling: Animals were housed, handled, and cared for in strict accordance with the European Union Council Directives (2010/63/EU). The protocol was approved by the Committee on the Ethics of Animal Experiments Charles Darwin n°5.

Coating procedures: When needed, bottom surface areas of culture vessels were covered with 1 mg/ml polyethyleimine (PEI; weight average molar mass 750,000; #P3143, Sigma Aldrich) diluted in a pH 8.3 borate buffer solution (40 mM) (Rousseau et al., 2013). After at least 1-2 h at 37°C, culture vessels were washed 4 times with Dulbecco's phosphate buffered saline medium (PBS) before application of culture medium and cell seeding. We also used laminin (#11243217001, Sigma Aldrich) diluted in PBS as a coating (Sepulveda-Diaz et al, 2016) for experiments made with astrocytes.

Microglial cell cultures: Microglial cell were isolated from the brain of newborn mouse pups (post-natal day 1) using a simple culture procedure that allows spontaneous and selective isolation of these cells in bulk quantities (Sepulveda-Diaz et al, 2016). Briefly, the isolation was performed by plating mechanically dissociated brain cells in PEI-coated Corning T-75 flasks (Sigma Aldrich) containing DMEM supplemented with 10% FCS and antibiotics. After a single medium change for removing cellular debris at day 2 *in vitro*,

the cultures were kept as such for 14-16 more days until completion of microglial cell isolation. When needed, purified microglial cell cultures were maintained longer in culture flasks by completing the cultivation medium with a small aliquot of fresh medium. To produce subcultures, microglial cells were recovered by trypsin proteolysis using an EDTA (2 mM)-trypsin (0.05%) solution and seeded in PEI-coated 48 multi-well plates at a density of about 100,000 cells. The cultures were then maintained in N5 medium, a cerebrospinal fluid-like medium (Kaufman and Barrett, 1983). This medium was supplemented with 5% horse serum, 0.5% FCS, 5 mM glucose and 100 µM glycine. Cultures were maintained at 37°C under a humidified atmosphere of 95% air and 5% CO_2. These cultures were virtually free of astrocytes.

Astrocyte cultures: To produce cultures enriched in astrocytes, we used a protocol of isolation that differed to that described previously for microglial cells, in that the coating was laminin and the culture medium DMEM/F-12 nutrient mixture supplemented with 10% FCS and antibiotics. The growth of these cultures was stopped after 2 weeks, i.e., at a stage where >90% of the cultured cells are astrocytes. To produce subcultures, adherent cells were recovered by trypsin proteolysis as described previously for microglial cells and seeded at a density of about 100,000 cells in Nunc 48 multi-well plates coated with laminin and filled with N5 medium supplemented with serum. Experiments of stimulation were performed in confluent astrocyte cultures.

Purification of recombinant αS

Human αS was expressed in *Escherichia coli* using the pT7-7 expression plasmid and purified as described (Hoyer et al., 2002; Kaylor et al., 2005; González-Lizárraga et al., 2017). The recombinant protein was recovered in 20 mM HEPES, 150 mM NaCl, pH 7.4 and its purity assessed by SDS-PAGE electrophoresis. Protein samples were then applied to a Pierce spin column (#88275; Thermoscientific) to remove endotoxins potentially present as contaminants. The endotoxin concentration in protein eluates was constantly below the detection threshold (0.1 EU/ml) of the chromogenic Limulus Amebocyte Lysate assay (#88282; Thermoscientific).

Protein solutions were then filtered and centrifuged at 12,000× *g* for 30 min and the protein content of the supernatant measured at 280 nm with a Nanodrop 8000

Spectrophotometer (Thermofischer Scientific) using an extinction coefficient of 5600 cm^{-1} M^{-1}. The protein concentration was finally adjusted to appropriate concentrations.

Preparation of αS aggregates

To produce aggregates, recombinant αS samples were incubated at 37°C in an orbital shaker (Thermomixer comfort; Eppendorf; Montesson, France) set at 600 rpm. After 96 h of incubation, protein aggregates were harvested, then sonicated for 2 min using a Branson B3510-DTH ultrasonic bath (VWR International, Fontenay sous Bois, France), and kept at -20°C until further use as previously described (González-Lizárraga et al, 2017). The formation of amyloid-type cross-beta structures was confirmed with the Thioflavin-T fluorescence assay (LeVine et al, 1999). The presence of amyloid fibrils was was further demonstrated by Transmission Electron Microscopy (TEM) using samples (5 µl) that were deposited on carbon Formvar coated grids (Electron Microscopy Sciences, Hatfield, PA; FF100-Cu, 100 Mesh). After enhancing the contrast with 2% uranyl acetate in water for 5 min at room temperature, the preparations were examined using a Hitachi HT7700 electron microscope (Elexience, Verrières-le-Buisson) operating at 70 kV as described (Ndour et al, 2017).

Protein detection by immunofluorescence

Cultures were fixed with 4% formaldehyde in PBS (20 min, room temperature), washed once with PBS, and then incubated with antibodies against MAC-1 (1:1000 in PBS for 72 h), Iba-1 (1:500 in PBS-Triton 0.2% overnight), αS (1:500 in PBS or PBS-triton 0.05% overnight), or p47-phox/NADPH oxidase (NOX)2 (1:50 in PBS-triton 0.05%, overnight). When MAC1/Iba-1 double immunostaining was performed, MAC-1 and Iba-1 were detected, sequentially. When MAC-1 was detected along with αSa, αS was used either diluted in PBS or in PBS-triton 0.05%. Suitable Alexa-Fluor 488 and Alexa-Fluor 555 conjugated secondary antibodies (Invitrogen) were used at a concentration of 1:250. Nuclei of labeled cells were counterstained with 4',6-diamidino-2-phenylindole (DAPI; 5 µg/ml for 2 min). Fluorescent images were acquired using a Nikon TE 2000 inverted microscope (Nikon, Tokyo, Japan) equipped with an ORCA-ER digital cooled camera and the HCI imaging software. When needed, changes in immunofluorescent

signal intensities were quantified at the cellular level using protocols described previously (Sepulveda-Diaz et al, 2016).

Counts of DAPI$^+$ nuclei

Numbers of DAPI$^+$ nuclei were estimated by automated counting using an Arrayscan XTi workstation equipped with the HCS Studio 2.0 Software (ThermoScientific, Courtaboeuf, France).

Western immunoblotting

Microglial cells were first pretreated with pharmacological reagents and 2 h later with αSa. After 30 min (for p-AKT) and 24 h (for total AKT or GADPH) of αSa stimulation, cells were processed using a protocol described earlier by Santa-Cecília and colleagues (2016). Briefly, adherent cells were treated with a M-PER buffer (#78501; Invitrogen) containing a protease and phosphatase inhibitor cocktail (#78440; Invitrogen) and aliquots of lysates were recovered for protein quantification with a Nanodrop 8000 Spectrophotometer (Thermofischer Scientific). Equal amounts of protein lysates were then resolved on a 10% polyacrylamide gel (SDS-PAGE) before transfer to polyvinylidene difluoride membranes. Membranes incubated with primary antibodies against p-AKT (1:1000; 30 min.), AKT (1:1000; overnight) and glyceraldehyde 3-phosphate dehydrogenase (GAPDH; 1:2000; 2 h) were washed with a Tris-buffered saline Tween-20 solution and then incubated with a rabbit secondary IRDye antibody (LI-COR Biosciences, Lincoln, NE, USA). Blots were imaged using a LI-COR Odyssey infrared imaging system (LI-COR Biosciences) and quantitative analysis of stained bands was performed with the ImageJ software (dos-Santos Pereira et al., 2015).

Glutamate assay

Glutamate was assayed using the Amplex Red Glutamic Acid/Glutamate Oxidase Kit (#A12221; Invitrogen) according to the manufacturer's instructions. The quantification was carried out with 25 µl of culture medium and the fluorescent reaction product

resulting from glutamic acid oxidation was quantified using a SpectraMax M4 microplate reader (Molecular Devices, Sunnyvale, CA).

Measurement of [^{14}C]-Cystine uptake

Cystine transport was measured based on a protocol described by Tomi and colleagues (2002). Briefly, microglial cells exposed to test treatments for 2h at 37°C were then incubated for the next 30 min with 8 µM [^{14}C]-Cystine. The uptake was terminated by washing the cultures 3 times with ice-cold PBS. The radioactivity accumulated by cultured cells was released by treatment with distilled water and quantified by liquid scintillation counting.

Quantification of intracellular ROS levels

Intracellular reactive oxygen species (ROS) were assessed using the membrane permeable CellROX Deep Red Reagent (Invitrogen Life Technologies), as described elsewhere (Sepulveda-Diaz et al., 2016).

Statistical analysis

Experimental values expressed as mean ±S.E.M. were derived from at least two sets of independent experiments. Statistical analyses were performed with the SPSS software for Windows (version 20). All pairwise comparisons were made by one-way ANOVA followed by the Student-Newman-Keuls post hoc test.

Results

αSa stimulate glutamate release in microglial cell cultures

We measured the impact that a 24-hour treatment with monomeric αS (αSm) (70 µg/ml) or with αSa (15 and 70 µg/ml) had on the release of glutamate in PEI-isolated microglial cell cultures, using LPS (10ng/ml) as a reference inflammogen (Lu et al, 2008). A treatment with 15µg/ml αSa caused a small but non-significant increase in glutamate release. With 70µg/ml αSa, however, the release of glutamate was robustly and significantly increased ($p < 0.0001$ *vs* control) (Figure 1a).The impact of 70 µg/ml αSa on glutamate release was roughly equivalent to that produced by 10 ng/ml LPS ($p < 0.0001$

vs control). Importantly, a treatment of microglial cell cultures with 70 µg/ml αSm did not affect glutamate release, indicating that non-aggregated monomeric forms of αS had no influence on this process. TEM images shown in Figure 1b confirmed that amyloid fibrils were present in αS shaken samples, only (lower image).

Astroglial cells which are also known to promote inflammatory-type reactions during neurodegeneration (Liddelow and Barres, 2017), failed to release glutamate in response to αSa (70 µg/ml) (Figure 1c). A similar result was found when astrocytes were challenged with LPS (10 ng/ml).

To determine to what extent increases in glutamate release induced by αSa (70 µg/ml) or LPS (10 ng/ml) were related to changes in microglial cell numbers, we counted the number of $DAPI^+$ nuclei in cultures receiving or not these treatments (Figure 1d). We found that the number of $DAPI^+$ nuclei was slightly augmented by about 1.25- and 1.15-fold in αSa (70 µg/ml)- and LPS (10ng/ml)-treated cultures, respectively ($p < 0.001$ and $p < 0.05$ *vs* control).

We also evaluated the impact of αSa on microglial cells using other inflammation markers. αSa (70 µg/ml) stimulated the release of the prototypical inflammatory cytokine TNF-α with similar efficacy as LPS (10 ng/ml) ($p<0.001$ *vs* control) (Figure 1e). αSa also strongly enhanced the expression of the microglial activation marker Iba-1 in $CD11b^+$ cells (Figure 1f), indicating that the increase in glutamate release induced by the fibrillary forms of the protein was reflecting a more generalized inflammatory state in microglial cells.

αSa stimulate glutamate release in microglial cells through a receptor-mediated process.

We found that αSa were frequently co-localized with the immunofluorescence signal for the cell surface integrin CD11b, when the antibody against human αS was used without permeabilization (Figure 2a). Aggregates were virtually absent in microglial cell bodies in these conditions (Figure 2a). Intracellular aggregates of αS remained also scarce after permeabilization (unshown data), suggesting that the intrinsic

phagocytocytic activity of microglial cells was reduced in present culture conditions or alternatively that our antibody did not recognize particules that had been phagocytized.

The presence of aggregates close to plasma membranes was an indication that the induction of glutamate release by αSa was possibly mediated by activation of microglial cell membrane receptors. To address this point, microglial cells were exposed to αSa (70 µg/ml) in the presence or not of MAb mTLR2 (2.5 µg/ml), an antagonistic antibody for TLR2 receptors (Chen et al, 2015). In the same setting, we also tested the impact of JNJ (20 µM), a synthetic antagonist for purinergic P2X7 receptors (Letavic et al, 2013). Figure 2b shows that glutamate release induced by αSa was markedly reduced by each of the receptor antagonists JNJ and MAb mTLR2 ($p < 0.0001$). When MAb mTLR2 and JNJ were added concurrently to αSa-treated cultures, glutamate release returned below control values ($p < 0.0001$), indicating that both TLR2 and P2X7 receptors contributed to the release of the neurotransmitter in this setting. Note that in the absence αSa, the basal release of glutamate was almost totally abolished in cultures treated with the two receptor antagonists.

Consistent with this set of results, we found that specific agonists for TLR2 and P2X7 receptors, Pam3CSK4 (1 µg/ml) (St Paul et al, 2012) and BzATP (500 µM) (Young et al, 2007), respectively, led to robust stimulation of glutamate release in microglial cell cultures ($p < 0.0001$ *vs* control) (Figure 2c). As expected, MAb mTLR2 (2.5 µg/ml) largely antagonized the induction of glutamate release elicited by Pam3CSK4 ($p < 0.01$ *vs* PAM) whereas JNJ (20 µM) reduced that elicited by BzATP ($p < 0.001$ *vs* BzATP). When Pam3CSK4 and BzATP were added together to the cultures, the increase in glutamate release appeared to be stronger than with each individual treatment ($p < 0.0001$ *vs* control). In this situation, a combination of MAb mTLR2 and JNJ was required to produce a substantial reduction in glutamate release ($p < 0.0001$ *vs* BzATP + PAM).

Glutamate release induced by αSa in microglial cells occurs through activation of the X_c^- antiporter system

Next, we tested the possibility that αSa could stimulate glutamate release by activating the antiporter system Xc^-, a membrane protein that imports into the cells the amino acid L-cystine, the oxidized form of cysteine, and exports L-glutamate in a 1:1 ratio (Lewerenz et al, 2013; Soria et al, 2016). To test this possibility, we studied the

impact of the Xc^- inhibitor Sulfa (Shukla et al, 2011) on the release of glutamate induced by αSa. Figure 3a shows that the induction of glutamate release by αSa (70 µg/ml; $p < 0.0001$ *vs* control) was completely antagonized by Sulfa (50 µM; $p < 0.0001$ *vs* αSa). Note that basal glutamate release was also totally suppressed by Sulfa in the absence of αSa ($p < 0.0001$ *vs* control), suggesting that the spontaneous release of glutamate resulted from basal activation of the Xc^- system.

To confirm the implication of this transport system in the effect of αSa, we measured the uptake of [^{14}C]-L-cystine in the same experimental setting. Because of technical constraints imposed by the use of this radiolabeled compound, the uptake was assessed for only 30 min in cultures previously exposed for 2 h to test treatments. Figure 3b shows that the accumulation of [^{14}C]-cystine was strongly elevated in microglial cells that were exposed to αSa ($p < 0.0001$ *vs* control). Sulfa led to substantial reduction of this increase ($p < 0.0001$ *vs* αSa), confirming that aggregated forms of αS had the capacity to stimulate the Xc^- antiporter system in microglial cells. Note that basal [^{14}C]-cystine uptake was also significantly decreased by Sulfa in control cultures ($p < 0.01$ *vs* control).

Glutamate release induced by αSa in microglial cells results from a rise in intracellular oxidative stress.

We next tested whether activation of the Xc^- system and ensuing stimulation of glutamate release were due to a rise of intracellular oxidative stress in microglial cells. For that, we tested the impact of various antioxidants on glutamate release in αSa-treated cultures. Figure 4a shows that the increase in glutamate release induced by 70µg/ml αSa was largely reduced by DPI (1 µM) and totally abolished by APO (300 µM), i.e., two compounds that operate as inhibitors of the superoxide producing enzyme NOX (Lelli et al, 2013) (APO: $p < 0.0001$ *vs* αSa; DPI: $p < 0.001$ *vs* αSa). The cell permeable analog of vitamin E, TROL (10 µM) was found as efficient as APO in the present setting ($p < 0.0001$ *vs* αSa).

So, to further confirm that oxidative stress was implicated in the stimulatory effects that αSa exert on glutamate release in microglial cells, we measured intracellular ROS production using the membrane permeable fluorogenic probe CellROX Deep Red Reagent (Sepulveda-Diaz et al, 2016). As expected ROS production was enhanced by 70µg/ml αSa ($p < 0.0001$ *vs* control) in microglial cells (figure 4b,c) and prevented by

APO, DPI and TROL (APO, DPI, TROL: $p < 0.0001$ *vs* αSa), i.e., treatments reducing glutamate release in αSa-treated cultures (Figure 4b,c).

The neurotransmitter dopamine prevents glutamate release induced by αSa in microglial cells through D_1 receptor activation.

Next, we were interested in studying whether the neurotransmitter DA had an impact on the release of glutamate induced by αSa in microglial cell cultures. More specifically, we found that DA (10 µM) totally abolished the stimulatory action of αSa (70 µg/ml) on glutamate release ($p < 0.0001$ *vs* αSa) (figure 5a). Note that DA also suppressed basal glutamate release under control conditions ($p < 0.0001$ *vs* control).

We wished to further characterize the inhibitory action of DA on glutamate release induced by αSa in microglial cells. For that we tested the impact that specific D_1 and D_2 DA receptor agonists could have on this process. D_1 receptors being most generally coupled to Gs and cAMP production (Beaulieu and Gainetdinov, 2011), we also tested the impact of the adenylate cyclase activator FK on glutamate release. LY (2.5 µM), an inhibitor of phosphoinositide 3-kinase (PI3K) was also tested in this experimental context (figure 5b). We found that the D_1 DA receptor agonist SKF-81,297 (10 µM) was able to mimic the inhibitory action of DA on glutamate release ($p < 0.0001$ *vs* αSa) whereas the D_2 agonist ERG (10 µM) failed to do so. We also established that FK (10 µM) led to substantial but only partial reduction of glutamate release in response to αSa exposure ($p < 0.001$ *vs* αSa) whereas LY (2.5 µM) had a strong inhibitory action under the same conditions ($p < 0.0001$ *vs* αSa).

This last observation prompted us to study expression levels of p-AKT, the enzymatic product of PI3K, using a Western blotting approach. In particular, we compared conditions in which αSa was applied alone or in the presence of DA, FK or LY to microglial cell cultures (Figure 5c). Quantitative Western blot analysis revealed that the expression of p-AKT was induced by αSa ($p < 0.05$ *vs* control) and this effect was prevented by either DA ($p < 0.001$ *vs* αSa) or FK ($p < 0.001$ *vs* αSa) (figure 5d). As expected, LY also robustly inhibited p-AKT expression in microglial cell cultures exposed to αSa ($p < 0.0001$ *vs* αSa).

Dopamine prevents glutamate release induced by αSa in microglial cells through an antioxidant effect.

We wished to determine whether the reduction in glutamate release produced by DA in αSa-treated microglial cultures was possibly due to an antioxidant effect of the neurotransmitter. To do that, we measured intracellular ROS production in microglial cell cultures exposed to 70 µg/ml αSa in the presence or not of 10 µM DA (Figure 6a,b). In the same setting, we also tested the impact of the adenylate cyclase activator FK (10 µM) and that of the PI3K inhibitor LY (2.5 µM) on ROS production (Figure 6a,b). Most notably, we found that the increase in intracellular ROS production induced by αSa was totally abolished by DA (10 µM) ($p < 0.0001$ *vs* αSa). Note that DA also reduced ROS production below control levels in the absence of αSa ($p < 0.01$ *vs* control). Interestingly, ROS produced by αSa were also reduced by the PI3K inhibitor LY (2.5 µM) ($p < 0.01$ *vs* αSa) and the adenylate cyclase activator FK (10 µM) ($p < 0.05$ *vs* αSa).

Finally, we tested the possibility that DA could prevent αSa-mediated ROS production by inhibiting the expression of NOX2, the NOX isoform that is most abundant in microglia cells (Bedard and Krause; 2007). For that we measured cellular expression levels of the NOX2 p47phox subunit in cultures exposed to αSa in the presence or not of DA or FK. We also tested the impact of LY in this setting (Figure 6c,d). We established that p47phox expression was induced in αSa-treated microglial cultures ($p < 0.0001$ *vs* control) and that this induction was prevented when DA (10 µM) was added concomitantly to the cultures ($p < 0.0001$ *vs* αSa). Cyclic AMP elevation with FK (10 µM) caused a reduction in the induction of p47phox elicited by αSa ($p < 0.05$ *vs* αSa). Meanwhile, p47phox returned to basal levels in cultures exposed to αSa in the presence of LY (2.5 µM) ($p < 0.0001$ *vs* αSa). Overall, these data suggest that DA prevented PI3K-dependent activation of NOX2 by αSa. All these results are summarized in figure 7.

Discussion

Using a model system of post-natal microglial cells in culture, we established that aggregated (but not monomeric) forms of αS had the capacity to robustly stimulate glutamate release through a mechanism requiring concomitant activation of TLR2 and P2X7 receptors and sequential stimulation of the PI3K and NOX enzymes. The Xc^-

antiporter system appeared to be the final downstream effector for αSa-mediated glutamate release. Interestingly, the effects of αSa on glutamate release were antagonized by the neurotransmitter DA through a mechanism that involves D_1 DA receptors.

Aggregated but not monomeric forms of αS stimulate glutamate release in microglial cell cultures

The aggregation process of the synaptic protein αS represents one of the key pathological events in PD. It has been suggested that pathological forms of αS that diffuse and propagate in the brain parenchyma (Dijkstra et al, 2014; Bernis et al, 2015) may contribute to disease progression by favoring inflammatory-type reactions mediated by microglial cells (Couch et al, 2011). Here, we wished to evaluate the pro-inflammatory potential of amyloid fibrils of αS, using glutamate release as an activation marker of these cells. Our specific interest for this marker comes from the fact that glutamate has the potential to generate low-level excitotoxic insults (Lavaur et al, 2017) that may aggravate neurodegeneration in PD (Ambrosi et al, 2014).

Using a model system of purified microglial cell cultures, we established that amyloid fibrils of αS had the capacity to stimulate glutamate release in a concentration-dependent manner. We found that both TNF-α secretion and cellular expression of the microglial activation marker Iba-1 were also robustly enhanced in the same cultures, indicating that the stimulatory effect of αSa on glutamate release reflected a more generalized inflammatory state of microglial cells. This is coherent with previous reports reporting on the strong pro-inflammatory potential of αS fibrillary species (Zhang et al, 2005; Wang et al, 2015; Brück et al, 2016). More precisely, we showed that 70 µg/ml αSa had an impact on glutamate release that was equivalent to that of 10 ng/ml of LPS, a cell-wall component that operates as a protypical inflammogen for microglial cells (Barger et al, 2007; Sepulveda-Diaz et al, 2016). Note that in some culture settings, toxic effects of aggregated forms of αS have been reported at much lower concentrations (Zhang et al, 2005; Kim et al, 2013). Concentrations comparable to those used by us in the present study were, however, required in other paradigms (Hoffmann et al, 2016; Bussi et al, 2017). We have no definite explanation for such differences, which may be

attributable to different culture conditions and various procedures used to generate aggregated species of αS.

At variance to αSa, αSm were totally ineffective in promoting glutamate release in microglial cells in the same experimental setting. These observations are coherent with reports showing that the inflammatory potential of αS is dependent on the aggregation state of the protein (Hoffmann et al, 2016). Incidentally, the absence of effect of αSm confirms indirectly that the human recombinant αS that we prepared for this study was free of bacterial contaminants susceptible to induce glutamate release in microglial cells (Barger et al, 2007).

Another population of glial cells, the astrocytes, are also involved in inflammatory-type reactions during neurodegeneration (Liddelow and Barres, 2017). Like microglia, astrocytes possess the capacity to release glutamate in physiological and pathological conditions (Vesce et al, 2007; Montana et al, 2014). Thus, we tested whether αSa had the potential to stimulate the release of the neurotransmitter when applied to astrocyte cultures. Contrarily to our expectation, we did not observe an increase in glutamate release when astrocytes were challenged with αSa, which means that the stimulatory action of αSa on the release process was rather specific to microglial cells.

Importantly, the capacity of αSa to trigger glutamate release from microglia signifies that the excitotoxic process affecting substantia nigra DA neurons in PD may not simply result from an increased excitatory drive from subthalamic glutamatergic neurons as suggested before (Wallace et al. 2007; Lavaur et al, 2017) but also from a local rise of the neurotransmitter.

αSa-mediated glutamate release in microglial cells is mediated by activation of membrane receptors

The presence of αSa closely apposed to plasma membranes is coherent with the know ability of amyloid-like structures to bind to cell membrane components (Shrivastava et al, 2017). This was also an indication that the stimulatory action of protein aggregates on microglial glutamate release may result from an interaction with cell membrane signal transducing receptors. Supporting this view, we found that glutamate release induced by αS was largely reduced in the presence of an antagonistic

antibody for TLR2 (Chen et al, 2015), a receptor subtype that is presumably involved in PD-related brain inflammation (Watson et al, 2012; Kim et al, 2016). Our result is in agreement with data reported by Gustot and colleagues (2015) showing that αS amyloid fibrils can trigger inflammatory-type reactions through a TLR-2-dependent mechanism. Kim and colleagues (2013) have shown, however, that αS oligomers spontaneously secreted by a neuroblastoma cell line had the potential to activate TLR-2 in microglial cells whereas fibrils produced from recombinant αS were unable to do so. Such discrepancies may be due to structural heterogeneity of αS oligomeric and fibrillary species in between studies (Bousset et al, 2013: Kumar et al, 2017). Glutamate release induced by αSa was also significantly curtailed by JNJ, a synthetic antagonist for purinergic P2X7 receptors (Letavic et al, 2013), which is reminiscent to previous studies showing that oligomeric forms of αS bind directly to this receptor subtype (Jiang et al, 2015). The implication of P2X7 receptors in the effects of αS fibrils has, however, not been reported previously.

Overall, these observations suggest that in our model system, both TLR2 and P2X7 receptors contributed to αSa-mediated glutamate release by microglial cells. Accordingly, a combined treatment with the TLR2 antagonistic antibody and the P2X7 antagonist JNJ was required to completely suppress the stimulatory action that αSa exert on glutamate release. Still in accord with our present finding, we found that glutamate release was stimulated by selective agonists of each receptor subtype, Pam3CSK4 and BzATP and that this stimulatory effect was further enhanced by a treatment combining the two agonist compounds.

αSa-mediated glutamate release in microglial cells results from an increase in intracellular oxidative stress

Next, we aimed to better understand the nature of the mechanisms that control glutamate release in microglial cells stimulated by αSa. Experiments showing that DPI and APO, two inhibitors of the NOX superoxide producing enzyme were able to suppress glutamate release induced by αSa, suggested that ROS contributed actively to the release process. TROL, a compound that inhibits hydroxyl radical-mediated lipid peroxidation was as efficient as the NOX inhibitors to prevent glutamate release,

indicating that superoxide-dependent hydroxyl radicals and/or lipid peroxyl radicals (Franzoni et al, 2006) operated as key mediators in this process. Quantitative detection of ROS with the membrane permeable fluorogenic probe CellROX confirmed that DPI, APO and TROL were all highly effective in preventing intracellular ROS production in microglia exposed to αSa. Note that glutamate release was also reported to be stimulated through NOX activation in microglial cells exposed to the bacterial inflammogen LPS (Barger et al, 2007) which indicates that intracellular events contributing to glutamate release in αSa- and LPS-treated microglial cells share comonalities.

In addition to that, we found that inhibition of PI3K with LY prevented the induction of ROS by αSa which is coherent with reports showing that both TLR2 (Lu et al, 2011) and P2X7 ligands signal through PI3K activation (Jiang et al, 2015). This also indicated that a PI3K-dependent mechanism controlled NOX activation in the present setting. Coherent with this view, the stimulation of microglial cells by αSa increased the immunofluorescent signal of p47phox, a subunit of NOX2, the NOX isoform that is predominant in microglial cells (Bedard and Krause; 2007). As expected this effect was totally reversed by PI3K inhibition, which is coherent with a previous report showing that PI3K controls NOX2 activation in microglial cells exposed to αS oligomers (Jiang et al, 2015). Still consistent with our results, Hou and colleagues (2018) reported that p47phox was robustly activated by αSa in microglial cultures. However, this effect which required activation of the CD11b integrin appeared not dependent on TLR-2 signaling.

The Xc^- cystine/glutamate antiporter system operates as downstream effector for αSa-mediated glutamate release

Note that we also observed that inhibition of αSa-mediated glutamate release by PI3K blockade was reproduced by Sulfa, an anti-inflammatory drug, which operates as inhibitor of the Xc^- cystine/glutamate antiporter system (Shukla et al, 2011). This suggested that Xc^- was possibly the final downstream effector for glutamate release stimulation by αSa in microglial cells. Comforting this view, the increase in glutamate release induced by αSa was accompanied by a concomitant rise in the uptake of L-cystine, a thiol aminoacid serving as precursor for the antioxidant defense tripeptide glutathione (GSH) (Lu, 2009). Cystine uptake appeared also largely antagonized by Sulfa,

confirming that the aminoacid was accumulated through the Xc^- antiporter. Given that several antioxidants also prevented glutamate release induced by αSa, one may assume that the increased activity of the antiporter was closely related to the induction of oxidative stress by aggregated forms of the protein.

The neurotransmitter dopamine prevents αSa-mediated glutamate release through an antioxidant effect

The loss of DA neurons and the ensuing depletion in brain DA is another key pathological feature of PD (Rodriguez-Oroz et al, 2009). Thus, we were interested in determining whether a deficit in DA could facilitate glutamate release induction by αSa. Consistent with this view, we found that DA was potently inhibiting glutamate release in cultures that were challenged with αSa. This result is reminiscent of previous observations showing that DA can reduce some of the inflammatory responses in microglia (Färber et al, 2005) and also in bone marrow-derived macrophages (Yan et al, 2015). The inhibitory effect of DA was entirely mimicked by a selective D_1 DA receptor agonist SKF-81,297 whereas ERG, an agonist at D_2 receptors failed to do so, indicating that DA effects resulted most probably from D_1 receptor activation. So, the possibility that DA could reduce the immunotoxicity of αS fibrils indirectly by forming complexes with them (Béraud et al, 2013) seemed rather unlikely. Note that DA reduced PI3K activation and ROS production in αSa-treated microglial cultures, which signifies that DA counteracted glutamate release stimulation by inhibiting PI3K-dependent signaling.

To mimic the effects of D_1 receptor activation in the present setting, we used the adenylate cyclase activator FK because this DA receptor subtype is coupled to cAMP production (Beaulieu and Gainetdinov, 2011). Even if being quite effective in reducing PI3K activation, FK caused only partial inhibition of the release of glutamate induced by αSa. This suggests that both canonical and non-canonical G protein coupling of D_1 receptors may occur in microglial cells. Coherent with this possibility, non-canonical G protein signaling has been reported in the immune system (Boularan and Kehrl, 2014).

Altogether, present data suggest that the activation of microglial cells by αSa may possibly contribute to a toxic build-up of extracellular glutamate in PD. The deficit in DA

that characterizes this disorder may further aggravate this process in a vicious circle mechanism.

Conflict of interests: The authors declare no competing interests

List of abbreviations: αS: α-Synuclein; αSa: αS aggregates; αSm: αS monomers; APO: Apocynin; BzATP: 2'(3')-*O*-(4-Benzoylbenzoyl)-ATP; DA: dopamine; DAPI: 4',6-Diamidino-2- Phenylindole; DMEM: Dulbecco's modified Eagle's medium; DPI: Diphenyliodonium; ERG: 2-bromo-α-ergocryptine; FCS: fetal calf serum; FK: forskolin; GAPDH: Glyceraldehyde 3-phosphate dehydrogenase; Iba-1: Ionized calcium binding adaptor molecule-1; JNJ: JNJ-47965567 or 2-(Phenylthio)-*N*-[[tetrahydro-4-(4-phenyl-1-piperazinyl)-2*H*-pyran-4-yl] methyl-3-pyridinecarboxamide; LPS: Lipopolysaccharide; LY: LY294002 or 2-(4-Morpholinyl)-8-phenyl-4*H*-1-benzopyran-4-one hydrochloride; NOX: NADPH oxidase; PBS: Dulbecco's phosphate buffered saline medium; PD: Parkinson's disease; PEI: polyethyleneimine; PI3K: Phosphoinositide 3-kinase; ROS: reactive oxygen species; Sulfa: sulfasalazine; TEM: Transmission electron microscopy; TLR: Toll-like Receptor; TROL: trolox.

Authors' contributions: MSP performed the experiments. MSP, LA, JR, SH, JSD, RRV and PPM contributed to the experimental design. JSD, FG, EDB, RC, RRV and PPM contributed with resources and materials. MSP, EDB, RRV and PPM wrote and edited the manuscript. MSP, JR, RRV and PPM performed data acquisition and analysis. All authors have approved the final manuscript.

Acknowledgments: The research leading to these results was supported by program Investissements d'Avenir [ANR-10-IAIHU-06] and the Translational Research Infrastructure for Biotherapies in Neurosciences [ANR-11-INBS-0011-NeurATRIS]. This work benefited from equipment and services from the CELIS and ICMQuant core facilities, at ICM. In particular, we wish to acknowledge expert assistance from David Akbar and Dominique Langui for inverted fluorescence microscopy and transmission electron microscopy, respectively. We wish to acknowledge helpful comments from Ana Carolina Issy, Keila Bariotto, Terence Duarte and Mariza Bortolanza.

References

Ambrosi, G., Cerri, S., Blandini, F. (2014) A further update on the role of excitotoxicity in the pathogenesis of Parkinson's disease. *Journal of Neural Transmission*, *121,* 849-59. https://doi.org/10.1007/s00702-013-1149-z

Barger, S. W., Goodwin, M. E., Porter, M. M., Beggs, M. L. (2007). Glutamate release from activated microglia requires the oxidative burst and lipid peroxidation. *Journal of Neurochemistry*, *101,* 1205-13. https://doi.org/10.1111/j.1471-4159.2007.04487.x

Bartels A. L., Willemsen A. T., Doorduin J., de Vries E. F., Dierckx R. A., Leenders K. L. (2010). [^{11}C]-PK11195 PET: quantification of neuroinflammation and a monitor of anti inflammatory treatment in Parkinson's disease? *Parkinsonism and Related Disorders*, *16,* 57-9. https://doi.org/10.1016/j.parkreldis.2009.05.005.

Beaulieu J. M., Gainetdinov R. R. (2011). The physiology, signaling, and pharmacology of dopamine receptors. *Pharmacological Reviews*, *63,* 182-217. https://doi.org/10.1124/pr.110.002642

Bedard, K., Krause, K. H. (2007). The NOX family of ROS-generating NADPH oxidases: physiology and pathophysiology. *Physiological Reviews*, *87,* 245-313. https://doi.org/10.1152/physrev.00044.2005

Béraud, D, Hathaway, H.A., Trecki, J., Chasovskikh, S., Johnson, D.A., Johnson, J.A., Federoff, H.J., Shimoji, M., Mhyre, T.R., Maguire-Zeiss, K.A. (2013) Microglial activation and antioxidant responses induced by the Parkinson's disease protein α-synuclein. *Journal of Neuroimmune Pharmacology, 8*, 94-117. https://doi.org/10.1007/s11481-012-9401-0

Bernis, M. E., Babila, J. T., Breid, S., Wüsten, K. A., Wüllner, U., Tamgüney, G. (2015). Prion-like propagation of human brain-derived α-synuclein in transgenic mice

expressing human wild-type α-synuclein. *Acta Neuropathologica Communications*, *3,* 75. https://doi.org/10.1186/s40478-015-0254-7

Bohlen, C. J., Bennett, F. C., Tucker, A. F., Collins, H. Y., Mulinyawe, S. B., Barres, B. A. (2017). Diverse Requirements for Microglial Survival, Specification, and Function Revealed by Defined-Medium Cultures. *Neuron*, *94*, 759-773. e8. https://doi.org/10.1016/j.neuron.2017.04.043

Boularan, C., Kehrl, J. H. (2014). Implications of non-canonical G-protein signaling for the immune system. *Cellular Signaling*, *26*, 1269-82. https://doi.org/10.1016/j.cellsig.2014.02.010

Bousset L, Pieri L, Ruiz-Arlandis G, Gath J, Jensen PH, Habenstein B, Madiona K, Olieric V, Böckmann A, Meier BH, Melki R. (2013) Structural and functional characterization of two α-synuclein strains. *Nature Communications, 4,* 2575. https://doi.org/10.1038/ncomms3575.

Braak, H., Del Tredici, K. (2017). Neuropathological Staging of Brain Pathology in Sporadic Parkinson's disease: Separating the Wheat from the Chaff. *Journal of Parkinson's Disease*, *7(s1)*, S73-S87. https://doi.org/10.3233/JPD-179001

Brück, D., Wenning, G. K., Stefanova, N., Fellner, L. (2016). Glia and α-synuclein in neurodegeneration: A complex interaction. *Neurobiology of Disease*, *85*, 262-74. https://doi.org/10.1016/j.nbd.2015.03.003

Bussi, C., Peralta, Ramos, J.M., Arroyo, D.S., Gaviglio, E.A., Gallea, J.I., Wang, J.M., Celej, M.S., Iribarren, P. (2017) Autophagy down regulates pro-inflammatory mediators in BV2 microglial cells and rescues both LPS and alpha-synuclein induced neuronal cell death. *Scientific Reports, 7,* 43153. https://doi.org/10.1038/srep43153

Chen, L., Xie, Z., Turkson, S., Zhuang, X. (2015). A53T human α-synuclein overexpression in transgenic mice induces pervasive mitochondria macroautophagy defects preceding

dopamine neuron degeneration. *The Journal of Neuroscience*, *35*, 890-905. https://doi.org/10.1016/j.nbd.2015.03.003

Couch, Y., Alvarez-Erviti, L., Sibson, N. R., Wood, M. J., Anthony, D. C. (2011). The acute inflammatory response to intranigral α-synuclein differs significantly from intranigral lipopolysaccharide and is exacerbated by peripheral inflammation. *Journal of Neuroinflammation*, *8*, 166. https://doi.org/10.1186/1742-2094-8-166

Croisier, E., Moran, L. B., Dexter, D. T., Pearce, R. K., Graeber, M. B. (2005). Microglial inflammation in the parkinsonian substantia nigra: relationship to α-synuclein deposition. *Journal of Neuroinflammation*, *2*, 14. https://doi.org/10.1186/1742-2094-2-14

Dijkstra, A. A., Voorn, P., Berendse, H. W., Groenewegen, H. J., Netherlands Brain Bank, Rozemuller AJ, van de Berg, W. D. (2014). Stage-dependent nigral neuronal loss in incidental Lewy body and Parkinson's disease. *Movements Disorders*, *29*, 1244-51. https://doi.org/10.1002/mds.25952

dos Santos Pereira, M., Sathler, M. F., Valli Tda, R., Marques, R. S., Ventura, A. L., Peccinalli, N. R., Fraga M. C., Manhães A. C., Kubrusly R. (2015). Long Withdrawal of Methylphenidate Induces a Differential Response of the Dopaminergic System and Increases Sensitivity to Cocaine in the Prefrontal Cortex of Spontaneously Hypertensive Rats. *PLoS One*, *10*, e0141249. https://doi.org/10.1371/journal.pone.0141249

Emmanouilidou, E., Elenis, D., Papasilekas, T., Stranjalis, G., Gerozissis, K., Ioannou, P. C., Vekrellis, K. (2011). Assessment of α-synuclein secretion in mouse and human brain parenchyma. *PLoS One*, *6*, e22225. https://doi.org/10.1371/journal.pone.0022225

Färber, K, Pannasch, U, Kettenmann, H. (2005) Dopamine and noradrenaline control distinct functions in rodent microglial cells. *Molecular and Cellular Neuroscience, 29,* 128-38. https://doi.org/10.1016/j.mcn.2005.01.003

Franzoni, F., Colognato, R., Galetta, F., Laurenza, I., Barsotti, M., Di Stefano, R., Bocchetti, R., Regoli, F., Carpi, A., Balbarini, A., Migliore, L., Santoro, G. (2006). An in vitro study on the free radical scavenging capacity of ergothioneine: comparison with reduced glutathione, uric acid and trolox. *Biomedicine & Pharmacotherapy*, *60*, 453-7. https://doi.org/10.1016/j.biopha.2006.07.015

Gagne, J. J., Power, M. C. (2010). Anti-inflammatory drugs and risk of Parkinson disease: a meta-analysis. *Neurology*, *74*, 995-1002. https://doi.org/10.1212/WNL.0b013e3181d5a4a3

Ginhoux, F., Greter, M., Leboeuf, M., Nandi, S., See, P., Gokhan, S., Mehler, M. F., Conway, S. J., Ng, L. G., Stanley, E. R., Samokhvalov, I. M., Merad, M. (2010). Fate mapping analysis reveals that adult microglia derive from primitive macrophages. *Science*, *330*, 841–845. https://doi.org/10.1126/science.1194637

González-Lizárraga, F., Socías, S. B., Ávila, C. L., Torres-Bugeau, C. M., Barbosa, L. R., Binolfi, A., Sepúlveda-Díaz, J. E., Del-Bel, E., Fernandez, C. O., Papy-Garcia, D., Itri, R., Raisman-Vozari, R., Chehín, R. N. (2017). Repurposing doxycycline for synucleinopathies: remodelling of α-synuclein oligomers towards non-toxic parallel beta-sheet structured species. *Scientific Reports*, *7*, 41755. https://doi.org/10.1038/srep41755

Gustot, A., Gallea, J.I., Sarroukh, R., Celej, M.S., Ruysschaert, J.M., Raussens, V. (2015) Amyloid fibrils are the molecular trigger of inflammation in Parkinson's disease. *Biochemical Journal, 471*, 323-33. https://doi.org/10.1042/BJ20150617

Hirsch, E. C., Breidert, T., Rousselet, E., Hunot, S., Hartmann, A., Michel, P. P. (2003). The role of glial reaction and inflammation in Parkinson's disease. *Annals of the New-York Academy of Sciences*, *991*, 214-28. https://doi.org/10.1111/j.1749-6632.2003.tb07478.x

Hoffmann, A., Ettle, B., Bruno, A., Kulinich, A., Hoffmann, A. C., von Wittgenstein, J., Winkler, J., Xiang, W., Schlachetzki, J. C. (2016). α-synuclein activates BV2 microglia

dependent on its aggregation state. *Biochemical and Biophysical Research Communications*, *479*, 881-886. https://doi.org/10.1016/j.bbrc.2016.09.109

Hou, L., Bao, X., Zang, C., Yang, H., Sun, F., Che, Y., Wu, X., Li, S., Zhang, D., Wang, Q. (2018) Integrin CD11b mediates α-synuclein-induced activation of NADPH oxidase through a Rho-dependent pathway. *Redox Biology*, *14*, 600-608. https://doi.org/10.1016/j.redox.2017.11.010

Hoyer, W., Antony, T., Cherny, D., Heim, G., Jovin, T. M., Subramaniam, V. (2002). Dependence of α-synuclein aggregate morphology on solution conditions. *Journal of Molecular Biology*, *322*, 383-93. https://doi.org/10.1016/S0022-2836(02)00775-1

Jiang, T., Hoekstra, J., Heng, X., Kang, W., Ding, J., Liu, J., Chen, S., Zhang, J. (2015). P2X7 receptor is critical in α-synuclein-mediated microglial NADPH oxidase activation. *Neurobiology of Aging*, *36*, 2304-18. https://doi.org/10.1016/j.neurobiolaging.2015.03.015

Kaufman, L. M., Barrett, J. N. (1983). Serum factor supporting long-term survival of rat central neurons in culture. *Science*. *22*, 1394-6. https://doi.org/10.1126/science.6857258

Kaylor, J., Bodner, N., Edridge, S., Yamin, G., Hong, D.P., Fink, A. L. (2005). Characterization of oligomeric intermediates in α-synuclein fibrillation: FRET studies of Y125W/Y133F/Y136F α-synuclein. *Journal of Molecular Biology*, *353*, 357-72. https://doi.org/10.1016/j.jmb.2005.08.046

Kim, C., Ho, D.H., Suk, J.E., You, S., Michael, S., Kang, J., Joong Lee, S., Masliah, E., Hwang, D., Lee, H.J., Lee, S.J. (2013) Neuron-released oligomeric α-synuclein is an endogenous agonist of TLR2 for paracrine activation of microglia. *Nature Communications, 4,* 1562. https://doi.org/10.1038/ncomms2534

Kim, C., Lee, H. J., Masliah, E., Lee, S.J . (2016). Non-cell-autonomous Neurotoxicity of α-synuclein Through Microglial Toll-like Receptor 2. *Experimental Neurobiology*, *25*, 113-9. https://doi.org/10.5607/en.2016.25.3.113

Kumar, H., Singh, J., Kumari, P., Udgaonkar, J.B. (2017) Modulation of the extent of structural heterogeneity in α-synuclein fibrils by the small molecule thioflavin T. *Journal of Biological Chemistry 292,* 16891-16903. https://doi.org/10.1074/jbc.M117.795617

Lavaur, J., Le Nogue, D., Lemaire, M., Pype, J., Farjot, G., Hirsch, E.C., Michel, P. P. (2017). The noble gas xenon provides protection and trophic stimulation to midbrain dopamine neurons. *Journal of Neurochemistry*, *142*, 14-28. https://doi.org/10.1111/jnc.14041

Lelli, A., Gervais, A., Colin, C., Chéret, C., Ruiz de Almodovar, C., Carmeliet, P., Krause, K.H., Boillée, S., Mallat, M. (2013) The NADPH oxidase Nox2 regulates VEGFR1/CSF-1R-mediated microglial chemotaxis and promotes early postnatal infiltration of phagocytes in the subventricular zone of the mouse cerebral cortex. *Glia, 61,* 1542-55. https://doi.org/10.1002/glia.22540

Lema Tomé, C. M., Tyson, T., Rey, N. L., Grathwohl, S., Britschgi, M., Brundin, P. (2013). Inflammation and α-synuclein's prion-like behavior in Parkinson's disease -is there a link? *Molecular Neurobiology*, *47*, 561-74. https://doi.org/10.1007/s12035-012-8267-8

Letavic, M. A., Lord, B., Bischoff, F., Hawryluk, N. A., Pieters, S., Rech, J. C., Sales, Z., Velter, A. I., Ao, H., Bonaventure, P., Contreras, V., Jiang, X., Morton, K. L., Scott, B., Wang, Q, Wickenden, A. D., Carruthers, N. I., Bhattacharya, A. (2013). Synthesis and Pharmacological Characterization of Two Novel, Brain Penetrating P2X7 Antagonists. *ACS Medicinal Chemical Letters*, *4*, 419-22. https://doi.org/10.1021/ml400040v

LeVine, H. 3rd. (1999). Quantification of beta-sheet amyloid fibril structures with thioflavin T. *Methods in Enzymology*, *309*, 274-84. https://doi.org/10.1016/S0076-6879(99)09020-5

Lewerenz, J., Hewett, S. J., Huang, Y., Lambros, M., Gout, P. W., Kalivas, P. W., Massie, A., Smolders, I., Methner, A., Pergande, M., Smith, S. B., Ganapathy, V., Maher, P. (2013). The cystine/glutamate antiporter system Xc- in health and disease: from molecular mechanisms to novel therapeutic opportunities. *Antioxidants & Redox Signaling*, *18*, 522-55. https://doi.org/10.1089/ars.2011.4391

Liddelow, S. A., Barres, B. A. (2017). Reactive Astrocytes: Production, Function, and Therapeutic Potential. *Immunity*, *46*, 957-967. https://doi.org/10.1016/j.immuni.2017.06.006.

Lu, S. C. (2009). Regulation of glutathione synthesis. *Molecular Aspects of Medicine*, *30*, 42-59. https://doi.org/10.1016/j.mam.2008.05.005

Lu, Y. C., Yeh, W. C., Ohashi, P. S. (2008). LPS/TLR4 signal transduction pathway. *Cytokine*, 42, 145–151. https://doi.org/10.1016/j.cyto.2008.01.006

Lu, C., Liu, L., Chen, Y., Ha, T., Kelley, J., Schweitzer, J., Kalbfleisch, J. H., Kao, R. L., Williams, D. L., Li, C. (2011). TLR2 ligand induces protection against cerebral ischemia/reperfusion injury via activation of phosphoinositide 3-kinase/Akt signaling. *Journal of Immunology*, *187*, 1458-66. https://doi.org/10.4049/jimmunol.1003428

McGeer, P. L., McGeer, E. G. (2008). Glial reactions in Parkinson's disease. *Movement Disorders*, *23*, 474-83. https://doi.org/10.1002/mds.21751

Mesci, P., Zaïdi, S., Lobsiger, C. S., Millecamps, S., Escartin, C., Seilhean, D., Sato, H., Mallat, M., Boillée, S. (2015). System xC- is a mediator of microglial function and its deletion slows symptoms in amyotrophic lateral sclerosis mice. *Brain*, *138*, 53-68. https://doi.org/10.1093/brain/awu312

Michel, P. P., Hirsch, E. C., Hunot, S. (2016). Understanding Dopaminergic Cell Death Pathways in Parkinson Disease. *Neuron*, *90,* 675-91. https://doi.org/10.1016/j.neuron.2016.03.038

Montana, V., Verkhratsky, A., Parpura, V. (2014). Pathological role for exocytotic glutamate release from astrocytes in hepatic encephalopathy. *Current Neuropharmacology*, *12*, 324-33. https://doi.org/10.2174/1570159X12666140903094700

Mouton-Liger, F., Rosazza, T., Sepulveda-Diaz, J., Ieang A, Hassoun, S-M., Claire E., Mangone, G., Brice, A., Michel, P.P., Corvol, J-C., Corti, O. (2018) Parkin deficiency modulates NLRP3 inflammasome activation by attenuating an A20-dependent negative feedback loop. *Glia*, *in press*

Mullin, S., Schapira, A. H. (2015). Pathogenic mechanisms of neurodegeneration in Parkinson disease. *Neurologic Clinics*, *33*, 1-17. https://doi.org/10.1016/j.ncl.2014.09.010

Ndour, P. A., Larréché, S., Mouri, O., Argy, N., Gay, F., Roussel, C., Jauréguiberry, S., Perillaud, C., Langui, D., Biligui, S., Chartrel, N., Mérens, A., Kendjo, E., Ghose, A., Hassan, M. M. U., Hossain, M. A., Kingston, H. W. F., Plewes, K., Dondorp, A. M., Danis, M., Houzé, S., Bonnefoy, S., Thellier, M., Woodrow, C. J., Buffet, P. A.; French Artesunate Working Group. (2017). Measuring the Plasmodium falciparum HRP2 protein in blood from artesunate-treated malaria patients predicts post-artesunate delayed hemolysis. *Science Translational Medicine*, *9,* pii: eaaf9377. https://doi.org/10.1126/scitranslmed.aaf9377

Ouchi, Y., Yagi, S., Yokokura, M., Sakamoto, M. (2009). Neuroinflammation in the living brain of Parkinson's disease. *Parkinsonism and Related Disorders*, *Suppl 3*, S200-4. https://doi.org/10.1016/S1353-8020(09)70814-4

Rees, K., Stowe, R., Patel, S., Ives, N., Breen, K., Clarke, C. E., Ben-Shlomo, Y. (2011). Non-steroidal anti-inflammatory drugs as disease-modifying agents for Parkinson's disease: evidence from observational studies. *Cochrane Database Systematic Reviews*, *11*, CD008454. https://doi.org/10.1002/14651858.CD008454.pub2

Rodriguez-Oroz, M. C., Jahanshahi, M., Krack, P., Litvan, I., Macias, R., Bezard, E., Obeso, J. A. (2009). Initial clinical manifestations of Parkinson's disease: features and pathophysiological mechanisms. *Lancet Neurology*, *8*, 1128-39. https://doi.org/10.1016/S1474-4422(09)70293-5

Rousseau, E., Michel, P. P., Hirsch, E. C. (2013). The iron-binding protein lactoferrin protects vulnerable dopamine neurons from degeneration by preserving mitochondrial calcium homeostasis. *Molecular Pharmacology*, *84*, 888-98. https://doi.org/10.1124/mol.113.087965

Santa-Cecília, F. V., Socias, B., Ouidja, M. O., Sepulveda-Diaz, J. E., Acuña, L., Silva, R. L., Michel, P. P., Del-Bel, E., Cunha, T. M., Raisman-Vozari, R. (2016). Doxycycline Suppresses Microglial Activation by Inhibiting the p38 MAPK and NF-kB Signaling Pathways. *Neurotoxicity Research*, *29*, 447-59. https://doi.org/10.1007/s12640-015-9592-2

Sepulveda-Diaz, J. E., Ouidja, M. O., Socias, S. B., Hamadat, S., Guerreiro, S., Raisman-Vozari, R., Michel, P. P. (2016). A simplified approach for efficient isolation of functional

microglial cells: Application for modeling neuroinflammatory responses in vitro. *Glia*, *64*, 1912-24. https://doi.org/10.1002/glia.23032

Shrivastava, A. N., Aperia, A., Melki, R., Triller, A. (2017). Physico-Pathologic Mechanisms Involved in Neurodegeneration: Misfolded Protein-Plasma Membrane Interactions. *Neuron*, *95*, 33-50. https://doi.org/10.1016/j.neuron.2017.05.026

Shukla, K., Thomas, A. G., Ferraris, D. V., Hin, N., Sattler, R., Alt, J., Rojas, C., Slusher, B. S., Tsukamoto, T. (2011). Inhibition of xc^- transporter-mediated cystine uptake by sulfasalazine analogs. *Bioorganic and Medicinal Chemistry Letters*, *21*, 6184-7. https://doi.org/10.1016/j.bmcl.2011.07.081

Soria, F.N., Zabala, A., Pampliega, O., Palomino, A., Miguelez, C., Ugedo, L., Sato, H., Matute, C., Domercq, M. (2016). Cystine/glutamate antiporter blockage induces myelin degeneration. *Glia*, *64*, 1381-95. https://doi.org/10.1002/glia.23011

St Paul, M., Barjesteh, N., Paolucci, S., Pei, Y., Sharif, S. (2012). Toll-like receptor ligands induce the expression of interferon-gamma and interleukin-17 in chicken $CD4^+$ T cells. *BMC Res Notes*, *5*, 616. https://doi.org/10.1186/1756-0500-5-616

Tomi, M., Hosoya, K., Takanaga, H., Ohtsuki, S., Terasaki, T. (2002). Induction of xCT gene expression and L-cystine transport activity by diethyl maleate at the inner blood-retinal barrier. *Investigative Ophthalmology and Visual Science*, *43*, 774-9.

Vesce, S., Rossi, D., Brambilla, L., Volterra, A. (2007). Glutamate release from astrocytes in physiological conditions and in neurodegenerative disorders characterized by neuroinflammation. *International Review of Neurobiology*, *82*, 57-71. https://doi.org/10.1016/S0074-7742(07)82003-4

Wallace, B. A., Ashkan, K., Heise, C. E., Foote, K. D., Torres, N., Mitrofanis, J., Benabid, A. L. (2007). Survival of midbrain dopaminergic cells after lesion or deep brain stimulation

of the subthalamic nucleus in MPTP-treated monkeys. *Brain*, *130*, 2129-45. https://doi.org/10.1093/brain/awm137h

Wang, S., Chu, C. H., Stewart, T., Ginghina, C., Wang, Y., Nie, H., Guo, M., Wilson, B., Hong, J. S., Zhang, J. (2015). α-Synuclein, a chemoattractant, directs microglial migration via H_2O_2-dependent Lyn phosphorylation. *Proceedings of the National Academy of Sciences of the United States of America*, *112*, E1926-35. https://doi.org/10.1073/pnas.1417883112

Watson, M. B., Richter, F., Lee, S. K., Gabby, L., Wu, J., Masliah, E., Effros, R. B., Chesselet, M. F. (2012). Regionally-specific microglial activation in young mice over-expressing human wildtype α-synuclein. *Experimental Neurology*, *237*, 318-34. https://doi.org/10.1016/j.expneurol.2012.06.025

Yan, Y., Jiang, W., Liu, L., Wang, X., Ding, C., Tian, Z., Zhou, R. (2015). Dopamine controls systemic inflammation through inhibition of NLRP3 inflammasome. *Cell*, *160*, 62-73. https://doi.org/10.1016/j.cell.2014.11.047

Young, M. T., Pelegrin, P., Surprenant, A. (2007). Amino acid residues in the P2X7 receptor that mediate differential sensitivity to ATP and BzATP. *Molecular Pharmacology*, *71*, 92-100. https://doi.org/10.1124/mol.106.030163

Zhang, W., Wang, T., Pei, Z., Miller, D. S., Wu, X., Block, M. L., Wilson, B., Zhang, W., Zhou, Y., Hong, J. S., Zhang, J. (2005). Aggregated α-synuclein activates microglia: a process leading to disease progression in Parkinson's disease. *The FASEB Journal*, *19*, 533-42. https://doi.org/10.1096/fj.04-2751com

Figure legends

FIGURE 1 Induction of glutamate release in microglial cells by αSa. (a) Impact of a 24-hour treatment with αSa (15 and 70 µg/ml) or αSm (70µg/ml) on the release of glutamate in microglial cell cultures. Comparison with a treatment with the bacterial inflammogen LPS (10 ng/ml). Data are means ±S.E.M (n = 6) ****p<0.0001 *vs* controls.

(b) TEM images showing the presence of αS amyloid fibrils under shaken conditions, only (lower image). Scale bar: 1 µm. (c) Impact of a 24-hour treatment with αSa (70 µg/ml) or LPS (10 ng/ml) on the release of glutamate in astrocyte cultures. (d) Quantification of $DAPI^+$ nuclei after exposure of microglial cultures to the same treatments as in (c). Data are means ±S.E.M (n = 6). *p<0.05, and ***p<0.001 *vs* controls. (e) Quantification of TNF-α release after exposure of microglial cultures to the same treatments as in (c). Data are means ±S.E.M (n = 6). ***p<0.001 *vs* controls. (f) Visualization of CD11b (red) and Iba-1 (green) immunofluorescent signals and DAPI counterstained (blue) nuclei in αSa (70 µg/ml)- or LPS (10 ng/ml)-treated microglial cell cultures in comparison to control conditions. Merged images illustrate the global impact of treatments towards microglial cells. Scale bar: 50 µm.

FIGURE 2 Glutamate release induced by αSa in microglial cells results from cell surface receptor activation. (a) Digitized images showing the presence of fibrillary aggregates in cultures of microglial cells exposed to αSa (70 µg/ml) for 24 hours. CD11b (red), αS (white) and DAPI counterstained nuclei (blue). Scale bar: 10 µm. (b) Modulation of the effects of αSa (70 µg/ml) on glutamate release in microglial cell cultures treated with the MAb mTLR2 antagonist (T; 2.5 µg/ml) or the P2X7 receptor antagonist JNJ (J; 20 µM), used separately or in combination. (c) Impact that treatments with Pam3CSK4 (PAM; 1 µg/ml), a specific agonist for TLR2 and BzATP (500 µM), a specific agonist for P2X7 receptors, exert on glutamate release. Modulation of the effects of Pam3CSK4 and BzATP by MAb mTLR2 and JNJ, respectively. Impact of a combined treatment with Pam3CSK4 and BzATP on glutamate release when JNJ and MAb mTLR2, are added concurrently to the cultures. Data are means ±S.E.M (n = 8). ****p < 0.0001 *vs* controls. $^{\#\#}$p < 0.01, $^{\#\#\#}$ p < 0.001 and $^{\#\#\#\#}$ p < 0.0001 *vs* corresponding inflammogen.

FIGURE 3 Glutamate release induced by αSa in microglial cells occurs through activation of the X_c^- antiporter system. (a) Impact that Sulfa (50 µM) exerts on glutamate release in microglial cell cultures exposed to αSa (70 µg/ml). Data are means ±S.E.M (n = 6). ****p <0.0001 *vs* controls and $^{\#\#\#\#}$p<0.0001 *vs* αSa-treated cultures. (b) Impact that Sulfa (50 µM) exerts on [^{14}C]-L-cystine uptake in microglial cell cultures exposed to αSa

(70 µg/ml). Data are means ±S.E.M (n = 4). **p<0.01 and ****p<0.0001 *vs* controls. ####p<0.0001 *vs* αSa-treated cultures.

FIGURE 4 Antioxidants prevent the release of glutamate induced by αSa. (a) Impact that αSa (70 µg/ml) exert on glutamate release in microglial cell cultures in the presence or not of the antioxidants TROL (10 µM), APO (300 µM) and DPI (1µM). Data are means ±S.E.M (n = 6). ****p<0.0001 *vs* controls; ###p<0.001 and ####p<0.0001 *vs* αSa-treated cultures. (b) Intracellular ROS production visualized with the fluorogenic probe CellROX Deep Red in microglial cells exposed to the same treatments as in (a). Scale bar: 20 µm. (c) CellROX fluorescence intensities measured in the same conditions as in (a). Data are means ±S.E.M (n = 10). ****p<0.0001 vs control; ####p<0.0001 vs αSa-treated cultures.

FIGURE 5 Dopamine prevents glutamate release induced by αSa in microglial cells through D_1 receptor activation. (a) Impact of DA (10 µM) on glutamate release induced by a 24 h-treatment with αSa (70 µg/ml). Data are means ±S.E.M (n = 6). ****p<0.0001 *vs* controls; ####p<0.0001 *vs* αSa-treated cultures. (b) Impact of the D_1 receptor agonist SKF (10 µM), the D_2 receptor agonist ERG (10 µM), the adenylate cyclase activator FK (10 µM) and the PI3K inhibitor LY (2.5 µM) on glutamate release induced by αSa (70 µg/ml) in microglial cell cultures. Data are means ±S.E.M (n = 6-8). ****p<0.0001 *vs* control; ###p<0.001 and ####p<0.0001 *vs* αSa-treated cultures. (c) Western blot analysis of pAKT (phosphorylated at Ser473) in microglial cells exposed to αSa (70 µg/ml) for 30 min in the presence or absence of SKF-81,297 (10 µM), FK (10 µM) or LY (2.5 µM). Comparison with the expression of total AKT and GAPDH in sister cultures exposed for 24 hours to the same treatments as before. (d) Western blotting quantification of p-AKT/AKT in the same conditions as before. Data are means ±S.E.M (n = 4). *p<0.05 *vs* controls; ###p<0.001 and ####p<0.0001 *vs* αSa-treated cultures.

FIGURE 6 Dopamine prevents glutamate release induced by αSa in microglial cells through an antioxidant effect. (a) Intracellular ROS production visualized with the fluorogenic probe CellROX Deep Red in microglial cells treated with αSa (70 µg/ml) for 24 hours in the presence or not of DA (10 µM), FK (10 µM) or LY (2.5 µM). Scale bar: 20 µm. (b) CellROX fluorescence intensities measured in the same conditions as in (a). Data

are means ±S.E.M (n = 8). **p<0.01 and ****p<0.0001 *vs* controls. #p<0.05, ##p<0.01 and ####p<0.0001 *vs* αSa-treated cultures. (c) Visualization of NOX2 p47phox subunit in αSa-treated microglial cultures exposed or not to DA, FK or LY. Scale bar: 20 µm. (d) Expression levels of p47phox in the same conditions as in (c). Data are means ±S.E.M (n = 12). ****p<0.0001 *vs* controls. #p<0.05 and ####p<0.0001 *vs* αSa-treated cultures.

FIGURE 7 Schematic drawing showing how αSa may stimulate glutamate release in microglial cells. Extracellular αSa stimulate both TLR2 and P2X7 receptors. This results in the activation of a PI3K-dependent signaling pathway that controls ROS production through the NOX enzyme. Enhancement of oxidative stress by αSa leads to the activation of the Xc^- antiporter, thus promoting glutamate release and L-Cystine uptake. Glutamate release induced by αSa is prevented by the inhibitor of the Xc^- antiporter Sulfa, the inhibitors of NOX, APO and DPI and the antioxidant TROL. DA and the D_1 DA receptor agonist SKF inhibit glutamate release induced by αSa through an antioxidant effect mediated by PI3K inhibition. The effects of DA and SKF are only partially mimicked with the cAMP-elevating agent FK.

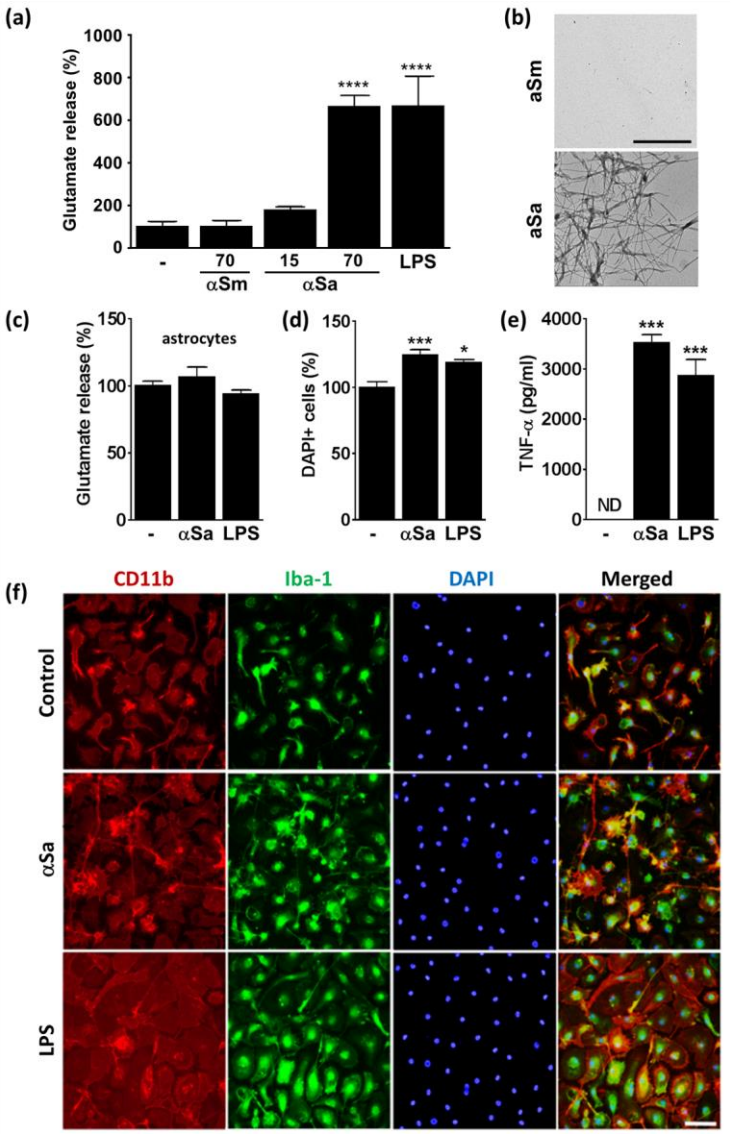
(a)
Glutamate release (%)
1000
800
600
400
200
0
****
****
-
70
αSm
15
70
αSa
LPS
(b)
aSm
aSa
(c)
astrocytes
Glutamate release (%)
150
100
50
0
-
αSa
LPS
(d)
DAPI+ cells (%)
***
*
(e)
TNF-α (pg/ml)
4000
3000
2000
1000
ND
***
***
(f)
CD11b
Iba-1
DAPI
Merged
Control
αSa
LPS

Figure 1

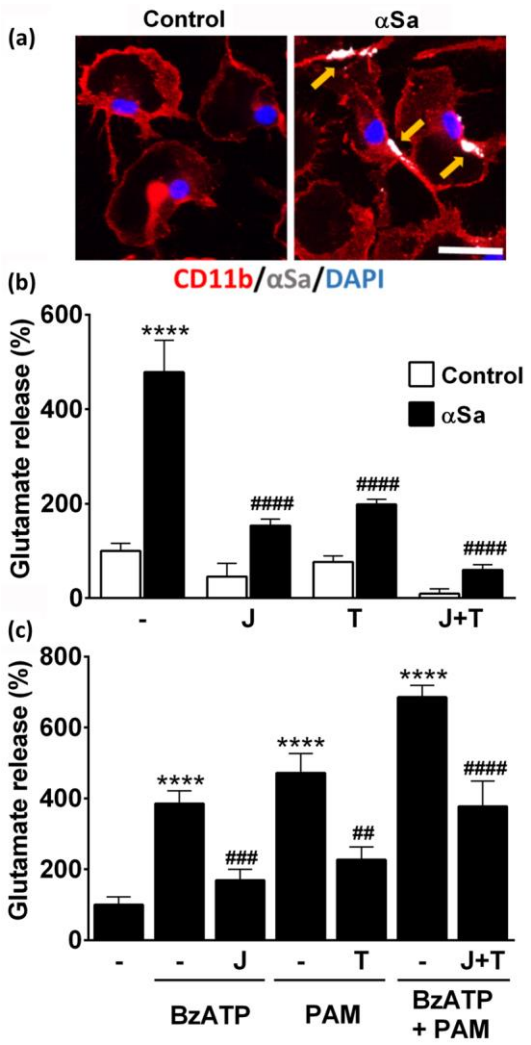
(a)
Control
αSa
CD11b/αSa/DAPI
(b)
Glutamate release (%)
600
400
200
0
****
####
####
####
Control
αSa
-
J
T
J+T
(c)
Glutamate release (%)
800
600
400
200
0
****
****
****
###
##
####
-
-
J
-
T
-
J+T
BzATP
PAM
BzATP
+ PAM

Figure 2

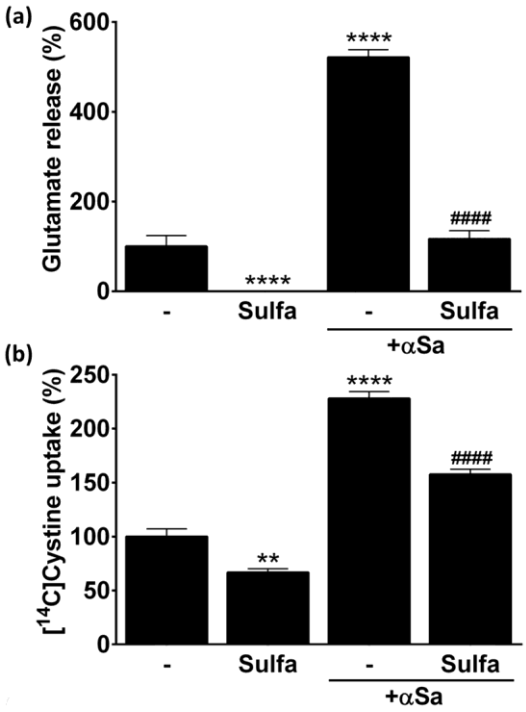
(a)
Glutamate release (%)
600
400
200
0
****
****
####
-
Sulfa
-
Sulfa
+αSa
(b)
[14C]Cystine uptake (%)
250
200
150
100
50
0
**
****
####
-
Sulfa
-
Sulfa
+αSa

Figure 3

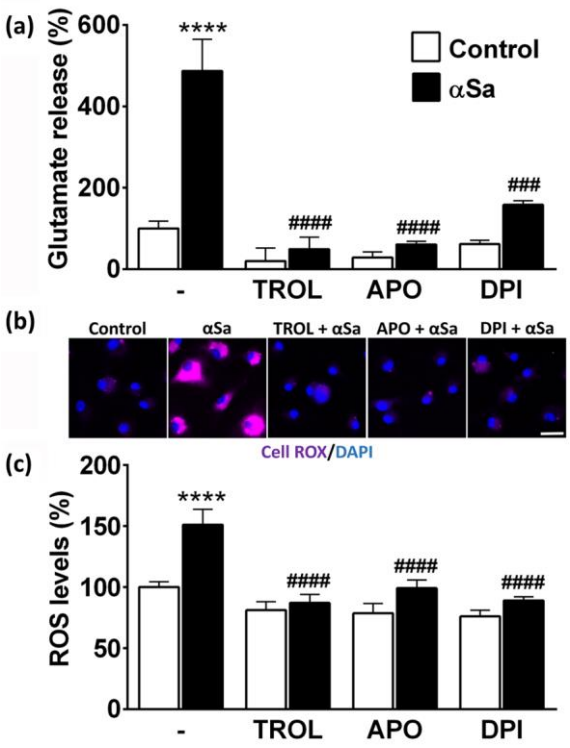
(a)
Glutamate release (%)
600
400
200
0
****
####
####
###
Control
αSa
-
TROL
APO
DPI
(b)
Control
αSa
TROL + αSa
APO + αSa
DPI + αSa
Cell ROX/DAPI
(c)
ROS levels (%)
200
150
100
50
0
****
####
####
####
-
TROL
APO
DPI

Figure 4

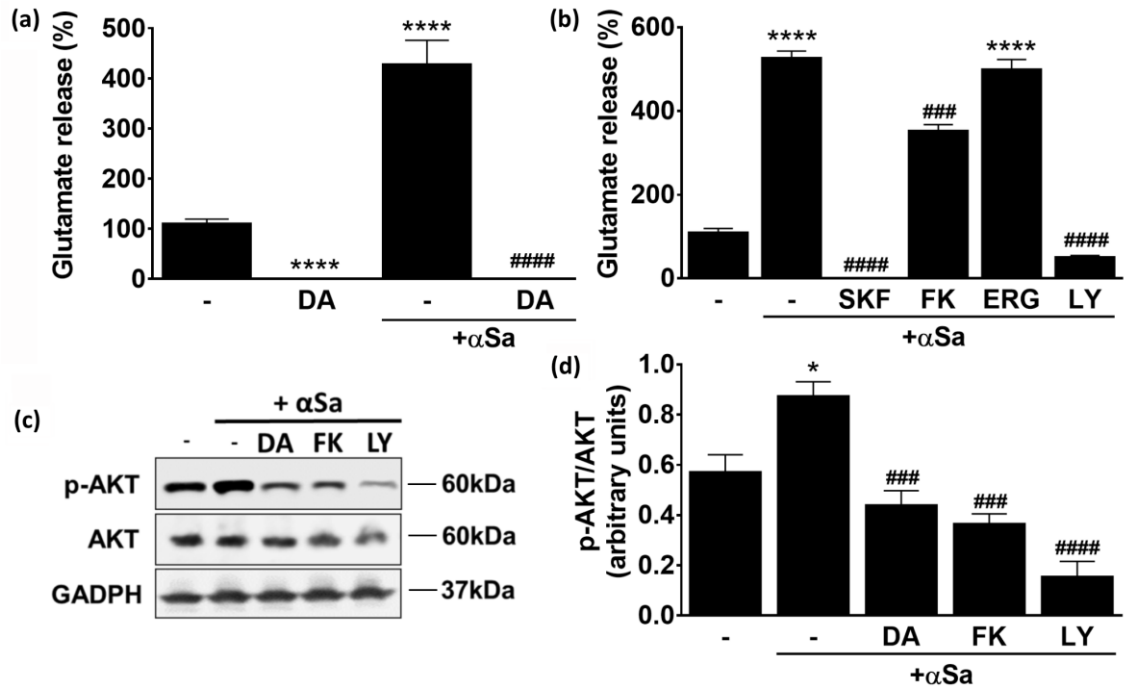
(a)
Glutamate release (%)
500
400
300
200
100
0
****
****
####
-
DA
-
DA
+αSa
(b)
Glutamate release (%)
600
400
200
0
****
####
###
****
####
-
-
SKF
FK
ERG
LY
+αSa
(c)
+ αSa
-
-
DA
FK
LY
p-AKT
AKT
GADPH
60kDa
60kDa
37kDa
(d)
p-AKT/AKT (arbitrary units)
1.0
0.8
0.6
0.4
0.2
0.0
*
###
###
####
-
-
DA
FK
LY
+αSa

Figure 5

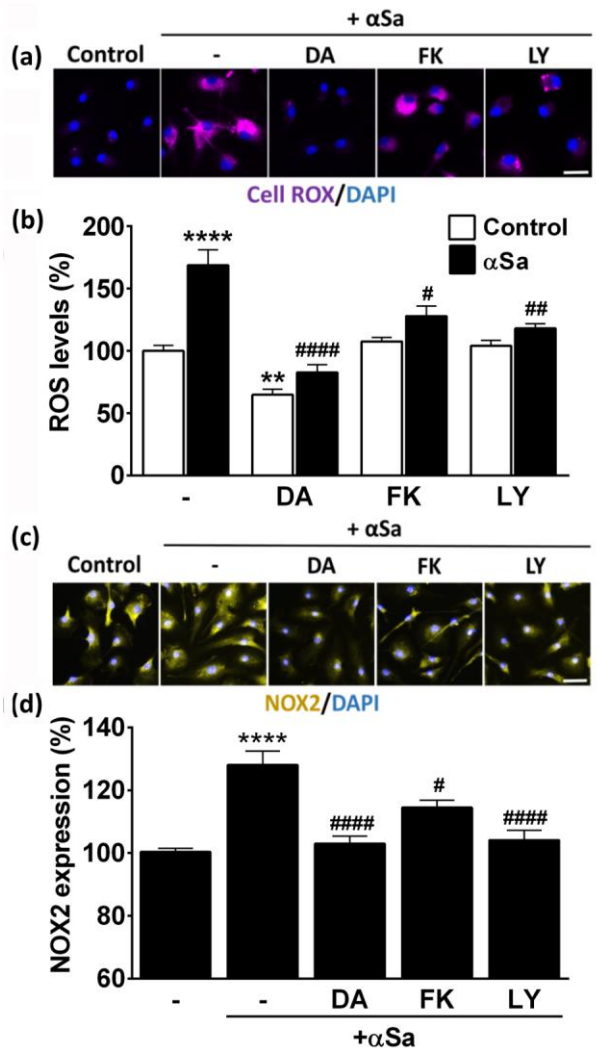
+ αSa
(a)
Control
-
DA
FK
LY
Cell ROX/DAPI
(b)
Control
αSa
ROS levels (%)
200
150
100
50
0
****
**
####
#
##
-
DA
FK
LY
(c)
+ αSa
Control
-
DA
FK
LY
NOX2/DAPI
(d)
NOX2 expression (%)
140
120
100
80
60
****
####
#
####
-
-
DA
FK
LY
+αSa

Figure 6

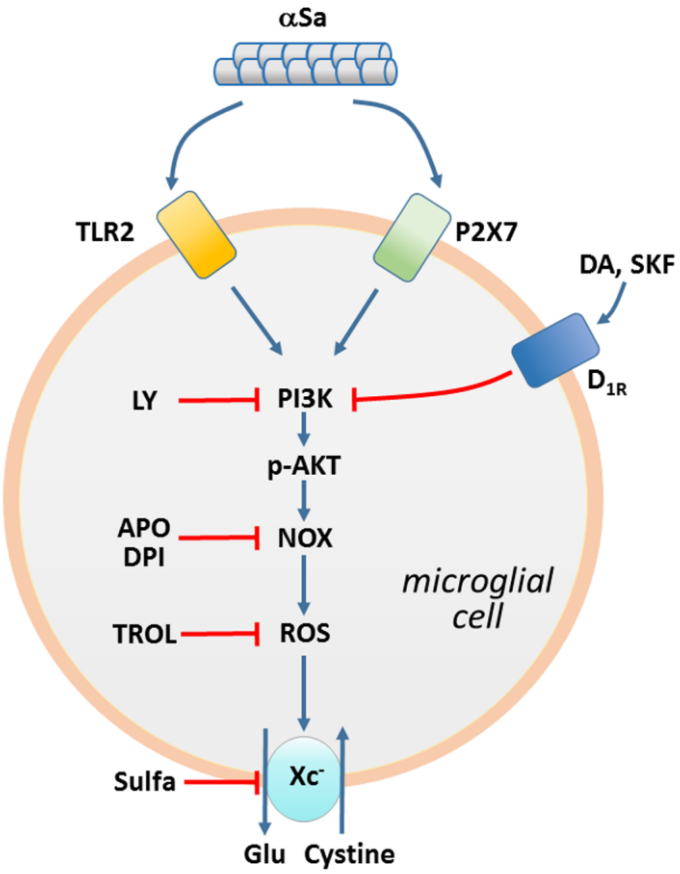
αSa
TLR2
P2X7
DA, SKF
D1R
LY
PI3K
p-AKT
APO
DPI
NOX
microglial
cell
TROL
ROS
Sulfa
Xc-
Glu
Cystine

Figure 7